PNAS RESEARCH ARTICLE | PSYCHOLOGICAL AND COGNITIVE SCIENCES

Structural features of the hippocampus covary with memory-guided attention depending on the side of hippocampal sclerosis

Gerardo Salvato[a,b,c,1], Gabriele De Maio[a,b,c], Claudio Bertolotti[b], Teresa Fazia[a], Pina Scarpa[b,c], Laura Tassi[d], Francesco Cardinale[d,e], Laura Castana[d], Silvia Amaryllis Claudia Squarza[f], Mariangela Piano[f], Manuela Bramerio[g], Martina Cerasetti[h], Eva Zita Patai[i], Anna Christina Nobre[j], Manuela Berlingeri[h,k], and Gabriella Bottini[a,b,c]

Affiliations are included on p. 11.

Edited by Daniel L. Schacter, Harvard University, Cambridge, MA; received February 19, 2025; accepted May 4, 2026

Past experiences stored in long-term memory (LTM) provide a valuable resource for making predictions that shape perception and guide goal-directed behavior. Contents from the high-capacity LTM system guide contextual selective attention to enhance sensory and higher-order processing of memory-predicted targets, in a process known as LTM-guided attention. While this essential cognitive function is believed to depend on the hippocampus, evidence is still scarce. In this study, we used a neuropsychological approach to test LTM-guided attention in the context of isolated hippocampal pathology and to explore structure-behavior covariance patterns. We tested healthy individuals (n = 20) and individuals suffering from focal epilepsy, with isolated, unilateral left (n = 20) or right (n = 17) hippocampal sclerosis (HS), in a task probing LTM-guided attention. Behavioral data indicated that individuals with left or right HS retained LTM-guided attention. We also assessed structure–behavior covariance using a multivariate structural neuroimaging approach. Hierarchical clustering analysis revealed that, in healthy individuals, LTM-guided attention performance covaried with atlas-derived subfield measures of the left hippocampal body. The volume of the left hippocampal body also covaried with attentional benefit in individuals with right HS. Interestingly, for individuals with left HS, LTM-guided attention covaried with the volume of the left hippocampus and with part of the right hippocampal volume. Together, these findings suggest that LTM-guided attention can be preserved in unilateral HS, with differences in hippocampal volume–behavior covariance depending on the side of hippocampal pathology.

attention | hippocampus | LTM-guided attention | epilepsy | long-term memory

Significance

Long-term memory helps us predict what is likely to happen in a familiar environment, allowing us to direct attention to relevant locations and objects. This form of memory-guided attention is believed to rely on hippocampal integrity. To test this hypothesis, we assessed individuals with unilateral hippocampal pathology and found that attentional benefits from learned context can remain preserved. Exploratory structural imaging analyses further indicated that individual differences in hippocampal volume are associated with variability in attentional guidance, depending on the location of hippocampal pathology. These findings highlight that memory can support attention even in the presence of focal hippocampal pathology, providing constraints on how adaptive cognitive processes are maintained when key memory structures are compromised.

Our perception of the world is strongly influenced by expectations. Past experiences stored as complex associative long-term memory (LTM) traces provide a rich source of predictions that proactively shape perception for goal-directed behavior (i.e., LTM-guided attention) (1–6). A growing body of evidence has demonstrated that a high-capacity memory system, such as the LTM, provides the essential elements for selective attention to guide and enhance perception by modulating early neural activity in favor of a memory-predicted target. Accordingly, LTM traces provide information about whether and how relevant events occur in a specific context, prioritizing the processing of crucial information. Such prospective and proactive premembering of experience (6) is essential in anticipating future demands and optimizing human performance.

Although the effects of LTM on perception are less well explored than those of short- and intermediate-term memory traces (6), they have been studied using a range of experimental approaches. Among these, memory-based orienting of attention tasks offer an ideal framework for investigating anticipatory biases based on LTM engrams. In one of these tasks, participants learn the associations between naturalistic scenes and everyday objects placed in specific locations within those scenes. After a variable amount of time, ranging from hours to days, participants are presented with learned naturalistic scenes and must detect the brief appearance of the associated object as quickly as possible. The initial scene presentation, without the embedded object, operates as a contextual cue, prompting memories of the associated object identity and location. Various memory-guided attention tasks show behavioral benefits in speed for identifying targets at remembered locations (7–13). Previous imaging studies show proactive, spatially specific modulation of visual areas during target anticipation, as well as engagement of dorsal frontoparietal attention-control regions and the hippocampus (7, 8, 12). In addition, behavioral findings

The authors declare no competing interest.

This article is a PNAS Direct Submission.

[1]To whom correspondence may be addressed. Email: gerardo.salvato@unipv.it.

This article contains supporting information online at https://www.pnas.org/lookup/suppl/doi:10.1073/pnas.2503466123/-/DCSupplemental.

Published June 22, 2026.

show a strong correlation between the quality of contextual memory and attention-related benefits in healthy young participants, suggesting a functional role of the explicit memory system in LTM-guided attention (7–12).

Indeed, LTM-guided attention seems to be supported by both declarative associative memory and attention-orienting cerebral networks [see for a recent review (14)], yet evidence in healthy populations is conflicting. Summerfield et al. (8) compared brain regions activated during memory-guided vs. visually-guided orienting of attention. In addition to engaging a common dorsal frontoparietal network typically reported in tasks of visually-guided attention, memory-guided attention further recruited a set of mainly left-lateralized regions, including the left hippocampus, left inferior frontal gyrus, left pulvinar, and the cerebellum bilaterally. Of these, activity in the left hippocampus co-varied on a trial-basis with the response-time benefits of memory-guided attention. Later, Stokes et al. (12) demonstrated the involvement of this region during the presentation of the cue scene rather than during target processing.

However, additional studies cast doubt on the role of the hippocampus. For instance, Rosen et al. (15) did not find hippocampal activation in a memory-guided change-detection task, whereas Günseli et al. (16) detected bilateral activation, although using a slightly different task. Importantly, a recent meta-analysis did not find hippocampal activation reliably associated with LTM-guided attention (14), raising questions about its role in attentional guidance. Finally, from a structural neuroimaging perspective, one study (17) proposed that both left and right hippocampal total volumes contribute to memory-guided attention in healthy populations, using the contextual cueing paradigm (18, 19). In this task, targets appearing consistently within repeating arrays are detected more rapidly, indicating implicitly learned spatial associations. Notably, contextual cueing may engage distinct cognitive mechanisms, as it relies on simpler stimulus arrays and involves learning and applying target–context associations on a shorter timescale, confined to task-specific settings.

Taken together, the mixed evidence for hippocampal engagement in LTM-guided attention has prompted several mechanistic hypotheses about its contribution to this complex cognitive function. One view proposes that the hippocampus forms and retrieves long-term contextual associations that support predictive signals. Through functional connections with attentional control regions, these spatial–contextual predictions are translated into anticipatory signals that bias sensory processing toward behaviorally relevant information (6, 8, 12). Alternatively, the hippocampal involvement during such tasks may reflect the explicit retrieval or recognition of repeated configurations (14, 20–22). This may occur implicitly, without requiring conscious access to the LTM trace during attentional guidance (10, 18, 19, 23, 24). A parsimonious account integrates these perspectives, positing that retrieval of spatial–contextual associations mediated by the hippocampus may serve both to orient attention and to support explicit recollection (25). At the same time, it remains possible that the two processes rely on partially independent mechanisms, with LTM-guided attention emerging from implicit contextual prediction.

Thus far, neuroimaging studies in healthy populations have produced conflicting, correlational evidence only. In contrast, the neuropsychological approach can test for the putative involvement of hippocampal structures in LTM- guided attention. The method involves exploring the relationship between a specific cerebral lesion and a behavioral deficit. Thus, investigating LTM-guided attention in clinical populations with selective hippocampal damage and declarative memory deficits can provide insights regarding the involvement of this structure in this vital cognitive function. To date, the pathological model has been interrogated exclusively through the contextual cueing paradigm, yet the cognitive mechanism underlying implicit contextual learning may engage different cognitive and neural processes than those underlying LTM-guided attention (6). Evidence in pathological populations is conflicting: Both neurodegenerative and nonneurodegenerative disorders have been reported to affect (26, 27) or not affect (28, 29) the contextual cueing advantage. A possible source of discord is the type of pathological population considered. Neurodegenerative diseases cause diffuse neuronal loss, offering limited insights into the contributions of specific regions. In contrast, studies involving temporal lobe lesions have relied on limited samples with nonspecific temporal lobe alterations (e.g., alterations in both hippocampi, including parahippocampal regions) or bilateral hippocampal damage (27). We believe that the most informative pathological model for LTM-guided attention would be selective unilateral hippocampal alterations and memory deficits without significant damage to other brain regions. Testing performance in memory-guided attention in a large, homogeneous sample in such clinical conditions would provide insights into the role of the hippocampus in LTM-guided attention.

Hippocampal Sclerosis (HS), associated with declarative LTM impairment, typically characterizes refractory temporal lobe epilepsy (TLE), which is the most frequent etiology of focal epilepsy in adults (30, 31). TLE is most commonly associated with declarative memory deficits, which affect about 70% of patients (32, 33). Interestingly, these deficits in patients with TLE and HS have been directly linked to specific HS patterns, depending on the number of cells damaged across hippocampal subfields. Coras et al. (34) demonstrated that declarative LTM impairments were associated with two patterns of neuronal loss: i) affecting all hippocampal subfields, including CA1, CA4, and dentate gyrus, or ii) predominant cell loss in CA4 and partially affecting also CA3 and dentate gyrus.

In this framework, testing LTM-guided attention in individuals with refractory TLE and isolated unilateral HS (left or right) offers a direct view into the role of mesial temporal lobe structures in this complex cognitive process. Accordingly, we recruited a sample of 37 individuals with TLE and left (N = 20) or right (N = 17) HS and a group of 20 healthy matched controls. Participants were tested with a modified version of a well-established LTM-guided attention task (7–12). Participants first learned the association between 72 everyday objects embedded in 72 realistic scenes. 30 min later, they performed an orienting of attention task in which they had to detect the brief appearance of the associated target object in the scenes from the initial learning task. Targets could appear at their learned location (i.e., valid trials) or a new location on the scene (i.e., invalid trials). Immediately after the orienting task, participants were tested on their explicit memory for the location and identity of the objects associated with each scene in the learning session. Participants also underwent a structural MRI scan. The pattern of association between atlas-derived hippocampal subfield volumes and behavioral outcomes was analyzed using hierarchical clustering, a commonly used methodology in cognitive neuroscience and neuropsychology to uncover multiscale brain–behavior organization (35–37). This approach was complemented with inferential statistics to formally test whether covariance patterns differed between groups.

Based on the available evidence, we predicted four potential patterns of results, depending also on the HS laterality: i) if LTM-guided attention relies on the left hippocampus (8, 12), the left HS (L-HS) group will show an impairment in LTM-guided attention compared to both healthy controls (HC) and the right

HS (R-HS) group; ii) if LTM-guided attention is supported by the hippocampi bilaterally (16), both L-HS and R-HS groups will show attention impairments in comparison with the HC group; iii) if no hippocampal activity is necessary for memory-guided attention (15), we will observe no behavioral differences among the three groups; iv) finally, if LTM-guided attention relies on the hippocampus but remains preserved despite hippocampal pathology, the HS groups may exhibit different patterns of association between memory-guided attention benefits and hippocampal volumetric estimates compared with HC. Such structure–behavior covariance patterns would suggest that variability in residual hippocampal anatomy relates to individual differences in attentional guidance following unilateral damage.

Results

Participants. The final sample was composed of 20 individuals with left (dominant hemisphere) HS (L-HS): 10 males, 10 females; age range 18 to 62, M = 36.950, SD = 11.83; years of education range 8 to 18, M = 12.5, SD = 2.373) and 17 with right (nondominant hemisphere) HS (R-HS: 6 males, 11 females; age range 23 to 54, M = 40.706, SD = 10.361; years of education range 8 to 16: M = 11.588, SD = 2.717). Demographic and clinical information are summarized in *SI Appendix*, Table S1. All patients included in this study had left or right HS identified by histopathologic assessment of their surgical specimens. Furthermore, Voxel-based Morphometry (VBM) analyses corroborated the presence of an isolated HS in both patients' groups (*SI Appendix*). 20 healthy individuals were also recruited as a control group (HC: 7 males, 13 females; age range 20 to 59, M = 41.55, SD = 12.181; years of education range 8 to 18, M = 13.250, SD = 2.633). Kruskal–Wallis tests showed no between-groups differences for age [$\chi^2_{(2)}$ = 1.923, P = 0.382, ε^2 = 0.034] or education [$\chi^2_{(2)}$ = 4.057, P = 0.132, ε^2 = 0.072]. The three groups were also matched for sex distribution [$\chi^2_{(2)}$ = 1.192, P = 0.551]. The R-HS and L-HS groups did not differ for disease duration (Mann–Whitney U test = 161.50, P = 0.807) and seizure frequency (Mann–Whitney U test = 148, P = 0.509).

Behavior.

Learning. In this first phase, participants learned the identity and location of commonly used objects embedded in realistic scenes (Fig. 1*A*). In each trial, they viewed an object, followed by a scene in which the same object was embedded. They searched for the target object and clicked it with the mouse cursor. Each unique scene was associated with a unique object appearing in a specific location. The object–scene pairings were repeated in random order over three blocks. For data analysis, we considered the percentage of correct responses (Search Accuracy) and the mean Search Times for object localization.

Accuracy in locating objects was high across all three groups and all blocks, averaging above 95% (Fig. 1*B*). A Generalized Linear Mixed Model (GLMM) was performed with Search Accuracy as the dependent variable, Group (HC, L-HS, R-HS) and Learning Block (1, 2, 3) as fixed factors, and subjects' ID as a random intercept. Because accuracy exhibited a ceiling effect, scores were transformed to yield a positively skewed distribution and then modeled with a gamma distribution using a logarithmic link function. Overall, the results showed high performance across all groups. Participants with R-HS were less accurate in the first

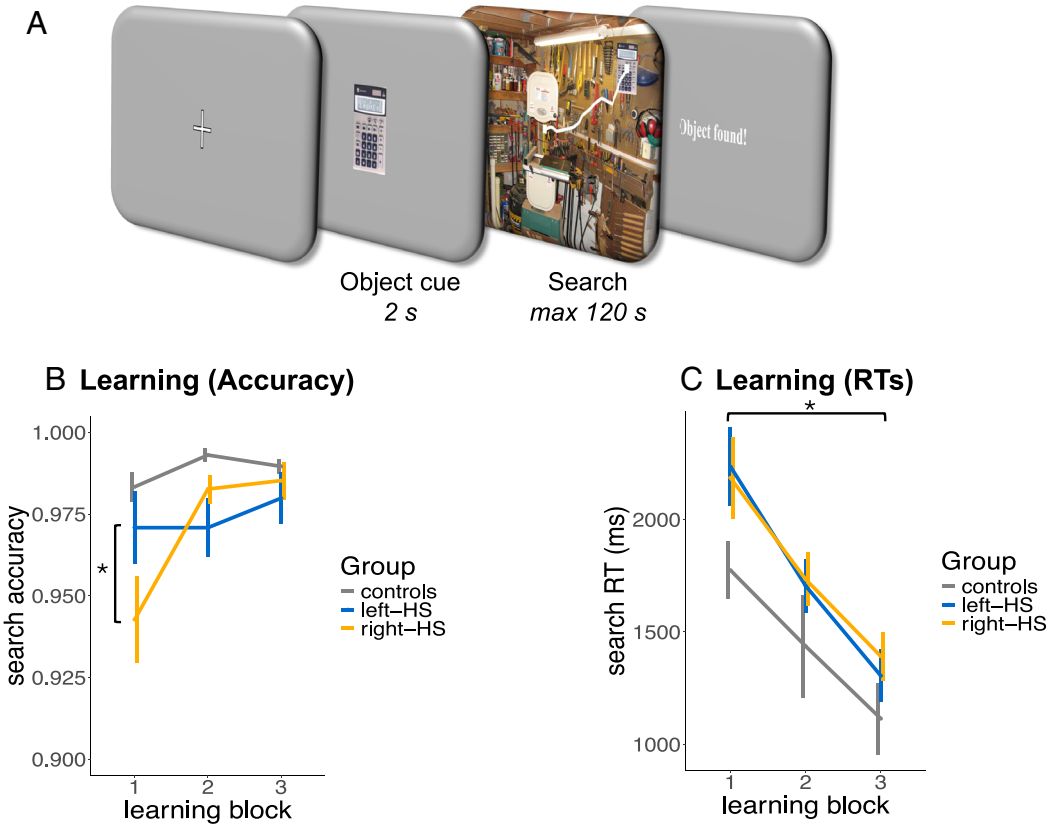

Fig. 1. Learning phase: experimental design and results. (*A*) Schematic illustration of the task structure. An everyday object was presented for 2 s. Then, a scene containing that object appeared. Participants had 2 min to find the target. (*B*) As learning blocks progressed, R-HS participants (in orange) showed significant improvement in accuracy, whereas both controls (in green) and L-HS participants (in blue) reached a ceiling. (*C*) Search Times showed the same linear decrease over the learning blocks for all participant groups. Error bars denote the SE of the means. Asterisks indicate P < 0.05.

block than in the other two blocks but showed improved accuracy over time. We found a significant main effect of Learning Block [$\chi^2_{(2)}$ = 35.214, P < 0.001; linear: z = 5.296; P < 0.001] and an interaction between Learning Block and Group [$\chi^2_{(4)}$ = 29.784, P < 0.001]. Probing the interaction revealed that Learning Block was significant only for the R-HS group (linear: z = −6.518; P < 0.001), indicating that participants with R-HS showed a significant improvement in accuracy across the blocks, whereas the other participants were close to the ceiling across all learning blocks (Fig. 1*B*). There was no main effect of Group [$\chi^2_{(2)}$ = 2.615, P = 0.280]. By the end of the learning phase, performance was equivalent and nearly 100% for all three groups, L-HS (M = 0.973; SE = 0.009), R-HS (M = 0.970; SE = 0.01), and HC (M = 0.989; SE = 0.008).

A GLMM was applied with Search Times as the dependent variable, Group (HC, L-HS, R-HS) and Learning Block (1, 2, 3) as fixed factors, and subjects' ID as a random intercept. A gamma distribution was used with a Logarithmic link function. Trials in which the object was not found during the three blocks of the learning task were excluded from this analysis (HC: 1.13%; L-HS: 2.62%; R-HS: 3.3%). The results indicated that search times decreased progressively and similarly for all three groups. A significant main effect of the Learning Block was found [$\chi^2_{(2)}$ = 169.804, $P \leqq 0.001$; linear z = −13.029, $P \leqq 0.001$], as all three groups showed decreasing search times as the blocks progressed. The main effect of Group [$\chi^2_{(2)}$ = 4.483, P = 0.106] and interaction Learning Block by Group [$\chi^2_{(4)}$ = 1.997, P = 0.736] were not significant. Overall, these results indicate a general learning effect, implying adequate engagement during the task.

LTM-Guided Attention. 30 min after the learning phase, participants performed the memory-guided attention task. The previously learned scenes were presented again (Fig. 2*A*). At first, the scenes were shown without the object, and after a variable interval, the associated object briefly flashed on the screen. Participants were instructed to click as quickly as possible upon seeing the object appear, regardless of its position. In eight trials (foil trials), a yellow hexagonal "STOP"

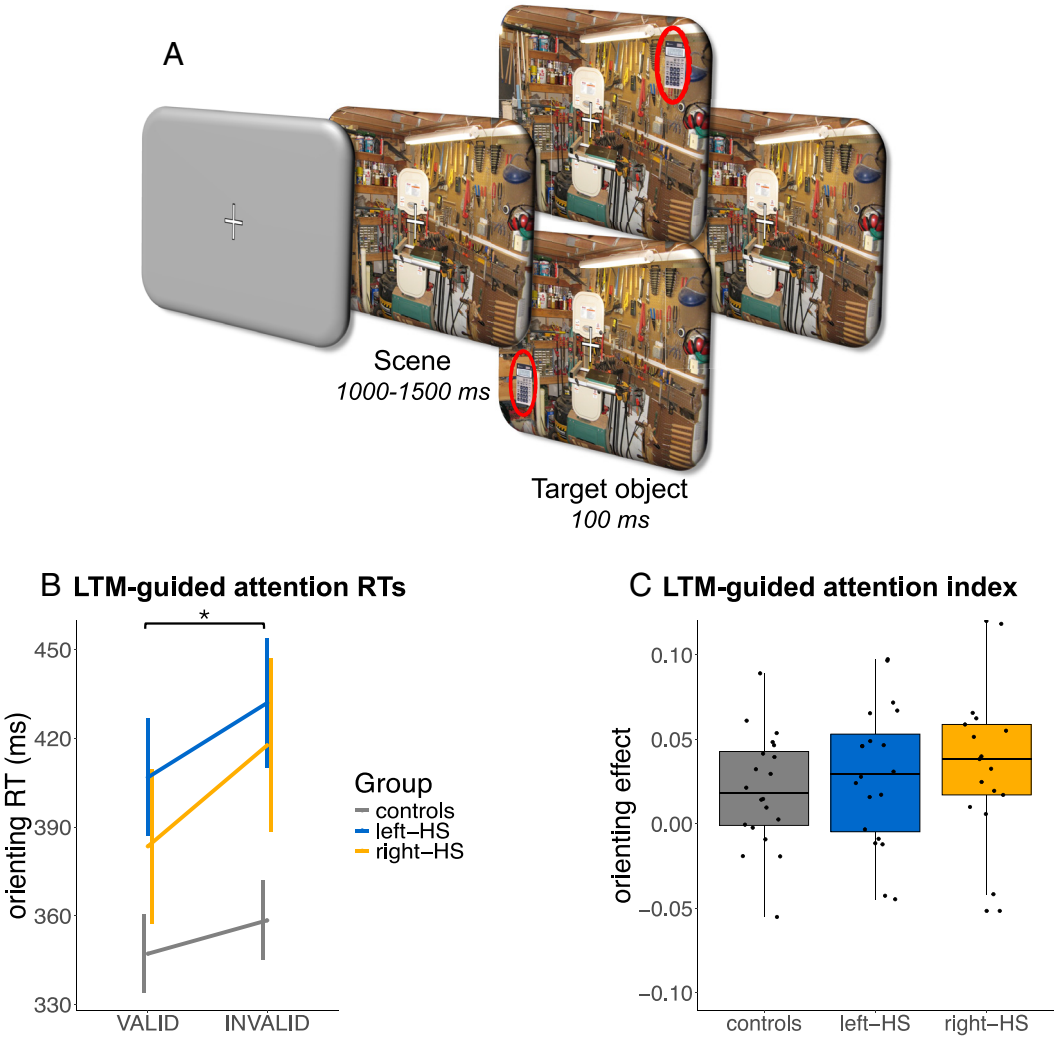

Fig. 2. LTM-guided attention: experimental design and results. (*A*) Schematic illustration of the orienting task structure. At the beginning of each trial, a scene previously associated with a target object appeared on the screen. After 1,000 to 1,500 ms, the target object briefly appeared on the scene in either a "valid" learned (here indicated in a red circle at the *Top* row) or in an "invalid" unlearned location (here indicated in a red circle at the *Bottom* row). Participants responded as soon as they saw the target object in the scene but refrained from responding when a foil (a yellow "STOP" sign) appeared. (*B*) Mean Reaction Times (RTs) for valid and invalid trials differed, with faster RTs in the valid condition. Error bars denote the SE of the means. Asterisks indicate P < 0.05. (*C*) The boxplots show the distribution of the LTM-based orienting index across the three groups. The central line indicates the median value (50th percentile), while the bounds of the box represent the 25th (lower bound) and 75th percentiles (upper bound), i.e., interquartile range (IQR). The whiskers extend to the minimum and maximum values within 1.5 times the IQR. Jittered points represent the individual data points. LTM-guided attention index showed no difference between groups.

sign appeared instead of the target object, and participants had to refrain from clicking. In half of the remaining trials, the target object appeared at the learned location (valid trials); in the other half, the target object appeared at a different location in other visual hemifields (invalid trials). Our primary measure of LTM-guided attention was the response time to detect the target in valid vs. invalid trials.

We ran a General Linear Mixed model with Validity (valid, invalid) and Group (HC, L-HS, R-HS) as predictors. Averaged RTs were inserted as the dependent variable, and the subjects' ID was used as a random intercept. Analysis of RTs showed significant and similar benefits of memory-guided orienting in the three groups (Fig. 2*B*). Results showed a main effect of Validity [$F_{(1,54)}$ = 30.361, P < 0.001; L-HS valid: M = 406.8 ms; SE = 19.9, invalid: M = 431.9 ms; SE = 19.9], R-HS valid: M = 381.4 ms, SE = 21.7, invalid: M = 411.6 ms, SE = 21.7; and HC valid: M = 347.1 ms, SE = 19.9, invalid: M = 360.7 ms, SE = 19.9. There was a tendency in the main effect of Group [$F_{(2,54)}$ = 2.839, P = 0.067], but no significant interaction Validity by Group [$F_{(2,54)}$ = 1.393, P = 0.257]. Furthermore, to ensure that the tendency for different response speeds between the three groups did not mask any qualitative difference in LTM-guided attention, we calculated a normalized measure as follows: [(RT invalid − RT valid)/(RT invalid + RT valid)]. The LTM-guided attention index was equivalent for HC group (M = 0.019, SE = 0.009), L-HS (M = 0.028, SE = 0.008), and R-HS (M = 0.037, SE = 0.009) [General Linear Model (GLM): $F_{(2,54)}$ = 0.835, P = 0.439, η^2_p = 0.03] (Fig. 2*B*). We supplemented these results with formal equivalence testing via the Two One-Sided Tests procedure, which confirmed that the orienting benefit in both HS groups was statistically equivalent to that of the HC group (*SI Appendix*). Given the simplicity of the task and the potential concern that participants might respond without perceiving or discriminating the target object, we also analyzed false alarms. There was no significant difference in the rates of false alarms [Kruskal–Wallis $\chi^2_{(2)}$ = 0.165, P = 0.920] for HC (M = 0.25, SD = 0.229), L-HS (M = 0.225, SD = 0.205), and R-HS (M = 0.279, SD = 0.288) groups, indicating they were equally able to inhibit their response to the foil stimulus. Finally, to investigate whether the laterality of the HS influenced LTM-guided attention based on the hemifield (left or right) of target appearance, we calculated two normalized indices of LTM-guided attention: [(RT invalid − RT valid)/(RT invalid + RT valid)], separately for left and right visual hemifields. The analysis revealed that the LTM-guided attention index was comparable between the L-HS and R-HS groups, regardless of the target side. A GLM analysis showed no significant main effect of group [$F_{(1,70)}$ = 1.301, P = 0.256, η^2_p = 0.02], no main effect of side [$F_{(1,70)}$ = 0.558, P = 0.457, η^2_p = 0.01], and no significant interaction between group and side [$F_{(1,70)}$ = 0.1724, P = 0.398, η^2_p = 0.01].

Explicit Retrieval. In the last phase of the experiment, participants' explicit memory content from the learning phase was assessed under two different conditions (Fig. 3*A*). Half of the learning trials assessed explicit memory for the object location and identity when cued by the scene ("Scene-cued"). The other half of the trials assessed object location and scene identity when cued by the object ("Object-cued"). To measure explicit contextual memory for object and scene identity, we examined the average accuracy in the two conditions. To measure explicit spatial contextual memory for object location within a scene, we compared the distance between the recalled location and the true object location.

Explicit memory for object and scene identity. To compare explicit contextual memory for object and scene identity between groups, we used accuracy in a four-alternative forced-choice (4AFC) task as the dependent variable in a GLM and Group as a predictor.

For the object identity (Fig. 3*A*), we found a main effect of Group [$F_{(2,53)}$ = 5.372, P = 0.008, η^2_p = 0.169]. Post-hoc Tukey corrected comparisons indicated that the L-HS group (M = 0.427, SE = 0.043) was less accurate than the HC group [M = 0.62, SE = 0.043; $t_{(53)}$ = −3.14, P = 0.008]. A tendency toward worse performance in the R-HS (M = 0.47, SE = 0.048) than in the HC group [$t_{(53)}$ = −2.306, P = 0.064] was observed. No difference was observed between the R-HS and L-HS groups [$t_{(53)}$ = −0.655, P = 0.79]. The three groups performed above the chance level (all Ps < 0.05)

For the scene identity (Fig. 3*B*), we found a main effect of Group [$F_{(2,53)}$ = 7.797, P = 0.001, η^2_p = 0.227]. Post-hoc Tukey corrected comparisons indicated that the L-HS group (M = 0.451, SE = 0.037) was less accurate than the HC group [M = 0.629, SE = 0.037; $t_{(53)}$ = −3.406 P = 0.004]. A similar decrement in performance occurred in the R-HS group (M = 0.442, SE = 0.041) relative to the HC group [$t_{(53)}$ = −3.368, P = 0.004]. No difference was observed between the R-HS and L-HS groups [$t_{(53)}$ = −0.156, P = 0.987]. The three groups performed above the chance level (all Ps < 0.05).

Explicit memory for object location. To compare explicit memory for the target object location, we used the pixel distance between the reported and actual locations of the object (*Materials and Methods*). We performed a GLM with distance in pixels as the dependent variable and Group as a predictor. No differences were found between groups for the scene-cued trials (Fig. 3*D*) [L-HS: M = 400.23, SE = 18.277; R-HS: M = 413.39, SE = 20.434, C: M = 356.91, SE = 18.277; $F_{(2,53)}$ = 2.441, P = 0.097, η^2_p = 0.084] or the object-cued trials [L-HS: M = 342.95, SE = 22.687; R-HS: M = 354.9, SE = 25.365, HC: M = 303.92, SE = 22.687; $F_{(2,53)}$ = 1.289, P = 0.284, η^2_p = 0.046; Fig. 3*E*]. We also compared explicit memory for the target object location, depending on whether the location response fell within the quadrant where the object had been learned. We performed a GLM with quadrant accuracy as the dependent variable and Group (HC, L-HS, R-HS) as a predictor. In the scene-cued trials, we found a main effect of group [$F_{(2,54)}$ = 5.6705, P = 0.006, η^2_p = 0.174]. Post-hoc Bonferroni corrected comparisons showed that L-HS (M = 0.368, SE = 0.031; P = 0.013) and R-HS (M = 0.334, SE = 0.034; P = 0.020) performed worse compared to HC (M = 0.497, SE = 0.31). No differences emerged between L-HS and R-HS (P > 0.05). In the object-cued trials, no between-groups differences emerged L-HS: M = 0.496, SE = 0.038; R-HS: M = 0.488, SE = 0.041, HC: M = 0.581, SE = 0.038; $F_{(2,54)}$ = 1.715, P = 0.190, η^2_p = 0.059.

LTM-Guided Attention and Explicit Contextual Memory. To test whether the quality of the memory trace for the association between object–scene identity and object spatial locations predicted the magnitude of the LTM-guided attention, and whether these associations differed between groups, we ran a GLM. The dependent variable was the LTM-based orienting index, and the predictors were Group (HC, L-HS, R-HS) and two memory measures: the average accuracy between object and scene identity tasks and the recalled mean distance of object spatial location averaged across both memory cued conditions. Results indicated that both memory measures predicted LTM-guided attention, with no group differences. There was a significant main effect of spatial distance [$F_{(1,47)}$ = 5.325, P = 0.025] and identity accuracy [$F_{(1,47)}$ = 5.936, P = 0.015]. Neither the main effect of

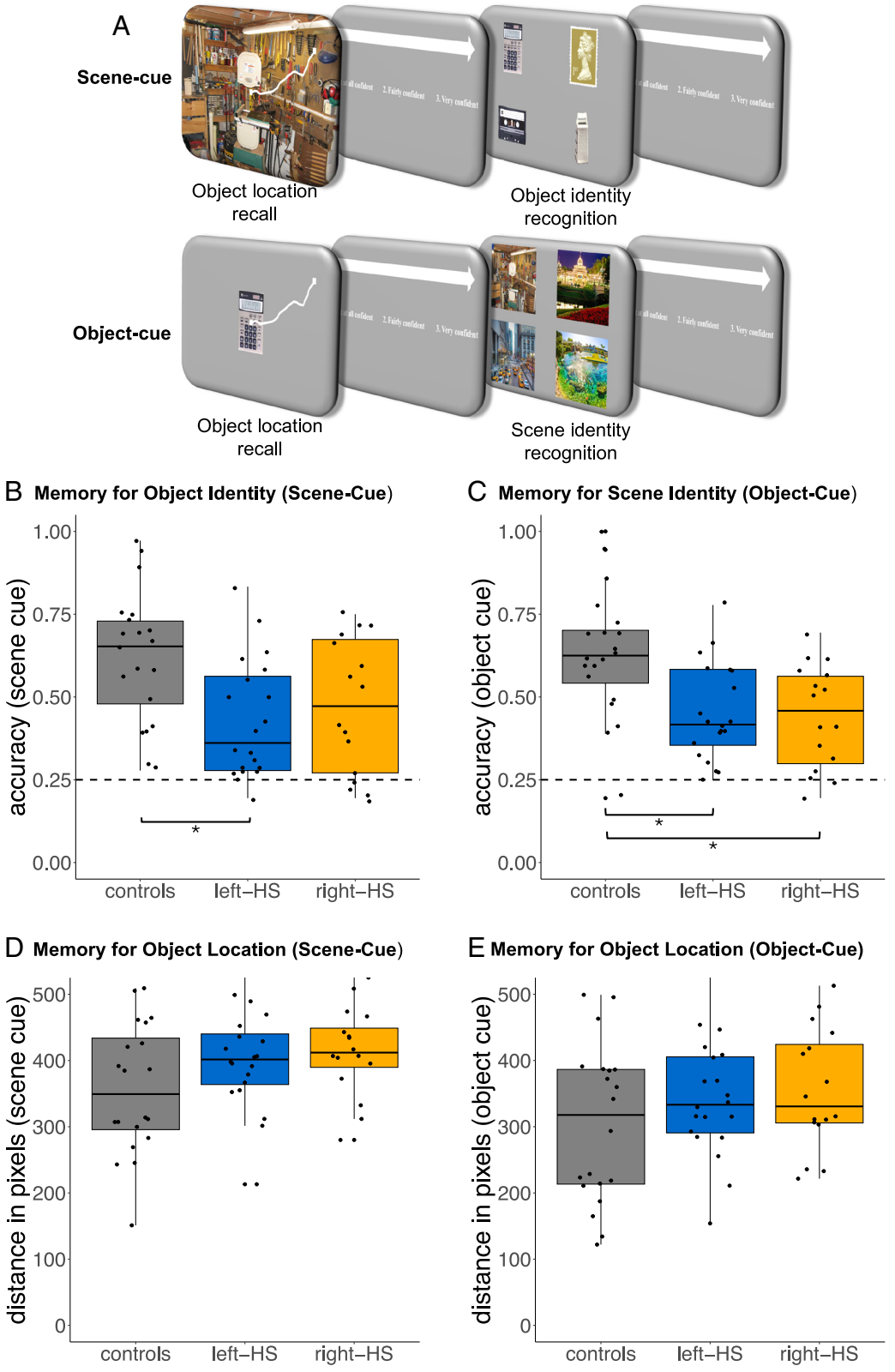

Fig. 3. Explicit retrieval: experimental paradigm and results. (*A*) Schematic illustration of the explicit retrieval task. In the "Scene-cue" condition, participants placed the mouse cursor at the spatial location of the object associated with a specific scene and estimated the confidence in their spatial memory performance. Then they chose the object associated with that scene and rated their confidence. In the "Object-cue" condition, participants placed the mouse cursor at the spatial location of the presented object and estimated the confidence in their spatial memory performance. Then they chose the scene associated with that object and rated their confidence. (*B*) Results of memory for object identity (Scene-cue). The Left-HS group was less accurate than the Control group. The dashed line indicates the chance level. (*C*) Results of memory for scene identity (Object-cue). Both left-HS and right-HS groups were less accurate than the Control group. The dashed line indicates the chance level. (*D*) Results of memory for object location in the Scene-cue condition. No difference between groups emerged. (*E*) Results of memory for object location in the Object-cue condition. Again, no difference between groups emerged. The boxplots show the distribution of the data across the three groups. The central line indicates the median value (50th percentile), while the bounds of the box represent the 25th (lower bound) and 75th percentiles (upper bound), i.e., IQR. The whiskers extend to the minimum and maximum values within 1.5 times the IQR. Jittered points represent the individual data points. Asterisks indicate $P < 0.05$.

Group [$F_{(2,47)}$ = 1.718, P = 0.191] or second-level interactions of Group by spatial distance [$F_{(2,47)}$ = 1.419, P = 0.252] or Group by identity accuracy [$F_{(2,47)}$ = 0.3877, P = 0.682] were significant. Results did not change when quadrant accuracy was used as a measure of spatial memory performance.

Covariance between Hippocampal Subfield Volumes and LTM-Based Attention. To explore patterns of structural covariance between the LTM-guided attention index and atlas-derived hippocampal subfield volumes, a hierarchical clustering analysis was performed for each group. This approach was complemented by inferential statistics to formally test whether covariance patterns differed significantly between groups. The LTM-based orienting index and the 16 hippocampal subfield volumes were included as variables (four subfields (CA1, CA2/CA3, CA4, DG), two hippocampal sectors (head, body) of the left and right hippocampus. In the HC group, the LTM-based orienting index showed structural covariance with the volumes of the CA1 and CA2/CA3 body of the left hippocampus. In the R-HS group, LTM-guided attention showed a covariance pattern with all subfields of the left hippocampal body. A different pattern emerged for the L-HS group, for whom the LTM-guided attention index covaried not only with the CA1 and CA2/CA3 body of the left hippocampus but also with all subfields of the right hippocampus, involving both the body and the head. For a visualization of the three different dendrograms, Fig. 4. For each of the three dendrograms, the clustering quality was quantified using the Davies–Bouldin (DB) index (38), which assesses cluster compactness and separation. DB values close to or below 1 typically indicate good clustering quality. The analysis showed that the HC and R-HS groups had a DB index of 1.4, while the L-HS group had a DB index of 1.1. These results suggest a generally good clustering quality, with well-separated clusters. Interestingly, as an additional control analysis, we repeated the hierarchical clustering using the amygdala (left and right nuclei). All three groups showed DB values indicating good clustering quality (HC = 0.389, L-HS = 0.434, and R-HS = 0.343). No structure-behavior covariance was observed between LTM-guided attention and amygdala subregions (*SI Appendix*).

Finally, to further explore the covariance patterns between hippocampal subfield volumes and LTM-guided attention, we conducted comparative analyses of the dendrograms derived from the three groups. We quantified the similarity between dendrogram structures across the three groups using the Baker-Hubert Gamma (BHG) index (39, 40), which evaluates the agreement between two sets of clusters by comparing the pairwise distances of data points within each clustering. We also assessed the statistical significance of similarities between the three dendrograms using a permutation approach with 10,000 iterations, in which group labels were randomly shuffled in each iteration. One-tailed P-values were calculated from the resulting empirical distribution. The comparison between HC and R-HS dendrograms showed moderate similarity (BHG index = 0.63, P = 0.68), providing insufficient evidence to conclude that the dendrograms differ significantly. In contrast, significant differences were observed between HC and L-HS (BHG index = 0.51, P = 0.0007) and between L-HS and R-HS (BHG index = 0.43, P = 0.0001). To visualize the differences between group datasets in hierarchical clustering, see also the tanglegrams in *SI Appendix*, Fig. S3.

Discussion

Here, we used a neuropsychological approach to examine whether LTM-guided attention relies on hippocampal integrity by testing whether individuals with unilateral HS exhibit deficits in orienting attention based on contextual LTM associations. Based on previous proposals, we considered whether the hippocampus may serve LTM-guided attention (6, 8, 12), explicit recollection (14, 20–22),

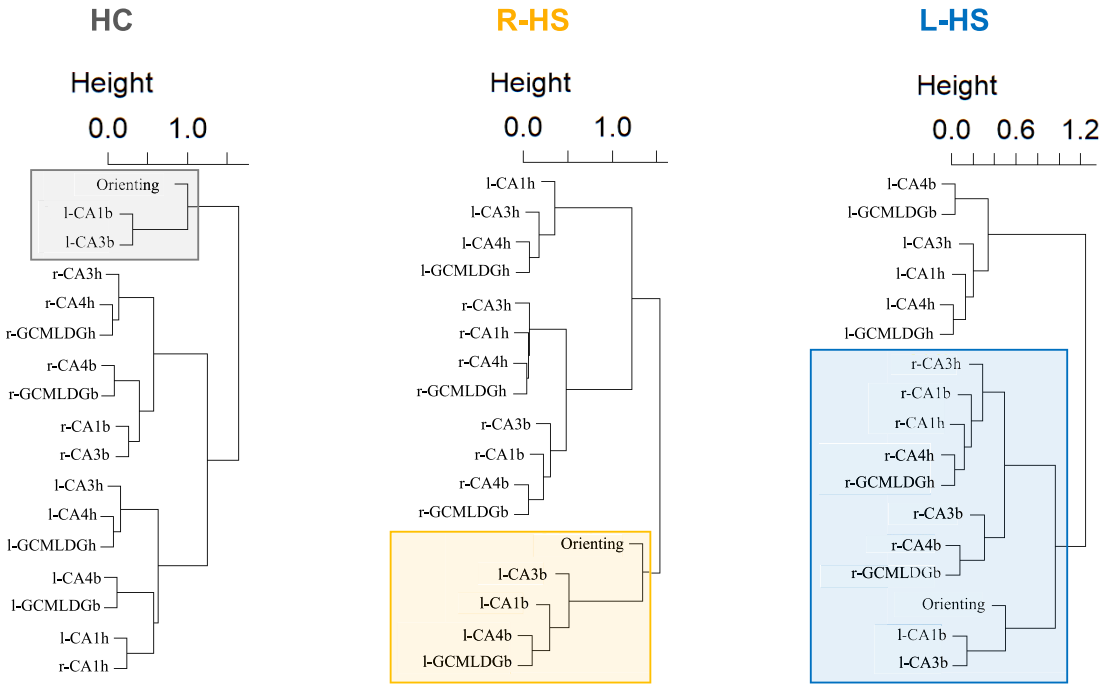

Fig. 4. Dendrograms. The figure presents cluster dendrograms for three groups. The *Left* section displays the dendrogram for HC, in which the LTM-based attention (Orienting) index clusters exclusively with the volumes of the CA1 and CA2/CA3 bodies of the left hippocampus. The *Middle* section illustrates the dendrogram for patients with R-HS, showing that the LTM-based orienting index clusters with all subfields of the left hippocampal body. Finally, the *Right* section depicts the dendrogram for patients with L-HS. Here, the LTM-based orienting index clusters not only with the CA1 and CA2/CA3 body of the left hippocampus but also with multiple subfields of the right hippocampus, including the head and body of CA1, CA2/CA3, CA4, and GCMLDG. Abbreviations: l- = left, r- = right, h = head, b = body, Orienting = LTM-guided attention index, GCMLDG = molecular and granule cell layers of the dentate gyrus.

or both (25). At the behavioral level, the data align with proposals that the hippocampus specifically supports explicit recollection (14, 20–22). Patients with left- and right-sided HS showed preserved LTM-guided attention despite deficits in explicit contextual memory recall. This dissociation suggests that the attentional orienting benefit may rely, at least in part, on mechanisms that are not strictly dependent on intact hippocampal-mediated explicit recollection. LTM-guided attention may not require conscious retrieval of episodic details at the time of attentional deployment but could be supported by implicit contextual prediction processes (10, 18, 19, 23, 24). By contrast, explicit retrieval of contextual associations appears to be more closely linked to hippocampal integrity. Such a dissociation between explicit and implicit memory-related processes is well established in the neuropsychological literature and has been documented in TLE patients (41–45) and, more specifically, in the context of LTM-guided attention. For example, in healthy aging, LTM traces can continue to bias attention even when older adults are less able to explicitly retrieve the associated contextual information compared with younger participants (10). Nevertheless, this interpretation remains speculative, as our task design did not directly assess participants' conscious access to the underlying memory representations during attentional guidance.

Importantly, however, in the presence of focal structural hippocampal damage, patients with HS may sustain cognitive performance through different mechanisms (41–43). Within the framework of functional brain activation, several fMRI studies have highlighted the involvement of the contralateral hippocampus during memory tasks in patients with unilateral TLE (46–53). For instance, Limotai et al. (50) in an fMRI study using an encoding task with complex scenes identified stronger activations in both left- and right-TLE patients in the contralateral hippocampus and parahippocampus, suggesting a compensatory mechanism for the detrimental effects of the pathology on cognition. Motivated by this line of evidence, but shifting from a neurofunctional to a structural neuroimaging approach, we interrogated the pathological model of unilateral, isolated HS to characterize the association pattern between left and right hippocampal volumes and behavioral indices of LTM-guided attention, using a data-driven hierarchical clustering approach.

The results of this analysis showed that the patterns of structure-behavior covariance significantly differed between groups. In healthy individuals, LTM-guided attention covaried with left hippocampal subregion volumes. This result was partially replicated in the R-HS group, in whom LTM-guided attention covaried with the volume of the body of all left hippocampus subfields. However, the clustering pattern in the L-HS group revealed differences in hippocampal structure–behavior covariance profiles relative to controls and patients with right HS: The LTM-guided attention measure covaried with atlas-derived subfield measures of left and right hippocampus volumes. Interestingly, we chose an anatomically close (but functionally distinct) region of control: the amygdala. The results of this control analysis showed that the LTM-guided attention index did not covary with the amygdala subregion volumes in the three groups. While these findings should be interpreted with caution, given the limited anatomical specificity afforded by the current imaging resolution, they nonetheless suggest that LTM-guided attention is associated with structural variability in the left hippocampus and, in particular, that covariance patterns differ across groups as a function of the side of hippocampal pathology.

Although the hemispheric specialization for cognitive functions is generally discussed in terms of verbal (left hemisphere) vs. visuospatial (right hemisphere) material specificity (54–56), there is evidence for the role of left hippocampal circuitry in nonverbal associative materials as well (57, 58). Regarding LTM-guided attention, previous studies have reported left hippocampal activation associated with attentional benefits driven by LTM traces (8, 12). Nevertheless, the role of the hippocampus in LTM-guided attention has been widely debated, as fMRI findings have yielded largely conflicting results. The divergent findings may be explained by differences in the experimental and statistical approaches. For example, Rosen et al. (15), who did not find hippocampal activity involvement, tested participants using a change-detection flicker task in which participants would learn and subsequently detect changes in natural scenes (e.g., removed tree, different windows in a building) and not associations between a target and its (spatial) context. The detection of the change may not have necessitated associative learning. Even if the repeated presentation of the scene enhanced perception, it may not have been sufficient to engage hippocampal activity to solve the task. In the study by Günseli and Aly (16), the bilateral hippocampal involvement might have arisen from a slightly different experimental paradigm and region of interest-based analyses. The authors sequentially presented images of 3D-rendered rooms, each with several pieces of furniture, unique wall-angle configurations, and a single painting. Participants had to indicate potential similarities between the presented images. Their data analysis focused on the roles of the hippocampus and ventromedial prefrontal cortex; thus, it was based on region of interest(s) that included both left and right hippocampi. Furthermore, the nature of the stimuli used (a naturalistic room) would have potentially triggered spatial navigation and thus activity in the right hippocampus.

Although we observed an association between left hippocampal subfield volumes and individual differences in LTM-guided attention, it is important to distinguish this structural covariance framework from fMRI-based functional activation evidence. Whereas prior neuroimaging studies have sought to identify task-related hippocampal engagement during attentional guidance, our volumetric findings offer a complementary, correlational perspective on how residual hippocampal anatomy may relate to preserved behavioral performance. Though suggestive, such structure–behavior covariance patterns cannot establish mechanistic functional recruitment or necessity of specific subfields on their own. This first piece of evidence set the rationale for further studies on this topic, unveiling the potential contribution of HS patients to a better understanding of the interplay between explicit associative memory and LTM-guided attention. Further investigations combining structural MRI and converging functional measures will be required to explicitly test whether attentional performance may remain intact following hippocampal pathology through multiple alternative mechanisms not directly assessed here by adopting structural imaging.

Moreover, in the current study, the presence of HS impaired performance on explicit memory tasks requiring the association of scenes with object identities—an effect particularly evident when patients were asked to recall the specific object–scene pairing. This deficit was less pronounced when the task required indicating the object location within the scene at pixel-level precision. However, when performance was analyzed categorically, based on whether the click fell within the correct quadrant of the screen, patients performed worse than controls, particularly when they viewed the scene without the object prior to indicating its location. One might speculate that the quadrant-based metric may introduce a threshold effect: Small positional deviations that cross quadrant boundaries are scored as categorical errors, thereby amplifying group differences that remain subtle in continuous distance measures.

In conclusion, the present study used a neuropsychological approach to examine LTM-guided attention in the context of unilateral HS. Across patient groups, we observed preserved orienting of attention effects despite impairments in explicit associative memory. We additionally explored multivariate structure–behavior relationships using hierarchical clustering, which suggested that individual differences in atlas-derived hippocampal volumetric estimates may covary with LTM-guided attention performance in a lateralized manner across groups. Notably, comparable associations were not observed in control regions such as the amygdala. These findings should be interpreted as descriptive and hypothesis-generating, rather than as evidence for mechanistic reorganization or definitive contralateral recruitment. Future studies in larger HS samples, combining morphometrical and neurofunctional measures will be important for determining how the structural covariance patterns observed in the current study reflect adaptive changes that support preserved attentional performance in the context of hippocampal pathology.

Materials and Methods

Participants. We recruited 37 consecutive individuals affected by refractory TLE and candidates for surgery at the "Claudio Munari" Epilepsy Surgery Centre of the ASST "Grande Ospedale Metropolitano" Niguarda in Milan, Italy. Participants were selected according to the following inclusion criteria: i) age between 18 y and 65 y old; ii) Mini-Mental State Examination [MMSE; (59)] over 24; iii) diagnosis of left or right TLE in the presence of HS; iv) absence of other diagnosed psychiatric or neurological pathologies; v) absence of other noncorrected primary sensory-motor diseases; vi) isolated left or right HS identified through the histopathologic assessment on the patients' surgical specimens; vii) absence of attentional deficits that could have adversely impacted the learning phase; viii) absence of any usual contraindications to MRI examination. The clinical sample consisted of 20 individuals with left HS and 17 with right HS. Twenty healthy individuals were also recruited for a control group (HC). For demographic and clinical information of the three groups, *SI Appendix*, Table S1. Informed consent was obtained before participation in the experiment. The study was approved by the Ethics Committee Milano Area 3 (number 666-17112020) and conducted in accordance with the Declaration of Helsinki.

Behavioral Paradigm.

Stimuli. We employed a modified version of a previously published experimental design (9, 10). Digital photographs of complex scenes and everyday objects served as visual stimuli. Colored photographs (1,000 × 750 pixels) of indoor and outdoor scenes were obtained from the Flickr Creative Commons (60, 61), while the objects were selected from the SUN dataset (62). 72 scenes and objects were used for the main task, with 12 additional scenes and objects used for familiarization and practice trials.

The object images were sized to fit within a 100 × 100 pixels transparent box (6.03° × 7.19°) when superimposed on the scene and a 150 × 150 pixels transparent box (9.04° × 10.77°) when presented against a black background. Each object was randomly assigned to one scene to create spatial object–scene associations. Two versions of each object–scene combination were prepared for counterbalancing: the target object was placed either on the left or right side of the scene. Across all scenes, objects were placed equiprobably in each of the four quadrants (upper left, lower left, upper right, and lower right). Objects were not necessarily semantically related to the associated scene, and their placement was not always realistic. The experiment involved three different phases: learning, LTM-guided attention, and explicit retrieval.

Task and Procedure.

Learning phase. In the first phase of the experiment, participants studied 72 pairings between unique scenes and objects. They were instructed to memorize the association between each scene and the identity and location of the embedded object (Fig. 1*A*). At the beginning of each trial, the target object was displayed at the center of the screen against a black background for 3 s. Subsequently, a full-screen scene containing the object was presented. Participants had to search for the target. Once they located the target, they clicked the left mouse button to activate a squared black cursor and then moved the mouse to click on the object. A maximum of 120 s was allotted to find the object. Positive feedback ("Object found") was provided for correct localizations, while negative feedback appeared for incorrect clicks or if the search time expired ("Object not found"). The 72 scene-object pairings were repeated over three consecutive blocks. Across blocks, the object–scene association and object position remained constant for each participant, while the presentation order of trials was randomized. To assess contextual learning across the three blocks, we measured the percentage of correct responses (Search Accuracy) and the mean Search Times for object localization. Search Times were calculated as the duration from the scene appearance to the first mouse click. Following the Learning phase, participants had a 30-min break during which they were instructed to relax and refrain from using any devices or materials that contained scenes or objects.

LTM-guided attention. Once the break ended, participants completed the LTM-guided attention task (Fig. 2*A*). All the scenes previously studied in the Learning phase were presented again in this part. To become familiar with the procedure, participants completed a 12-trial practice session before the main task, with a different set of scenes and objects. At the beginning of each LTM-guided attention trial, a fixation cross (1,000 to 1,500 ms) indicated that the scene was about to appear without any studied object. After a variable duration (1,000 to 1,500 ms), the associated object briefly appeared and then disappeared (100 ms), superimposed on the scene. Participants were asked to keep their gaze fixed on a fixation cross at the center of the screen and click as fast as possible when they saw the target object appear, regardless of its position. 64 trials were created based on the object–scene associations that participants had previously learned. For the remaining eight trials, a foil (a yellow hexagonal STOP sign with black lettering) appeared instead of the target object. Participants were asked not to click in this case. After the target or foil presentation, the scene disappeared after 1,000 ms, providing a response window, and the next trial began. No explicit memory retrieval was required to perform this LTM-guided attention task. However, the learned memory associations between the scene context and the item identity and location could implicitly facilitate target detection when the target location matched that in the previous Learning phase. For this reason, in half of the trials, the object (32 target objects and four foils) appeared at the originally learned location. In this valid condition, memory traces of the object location from the scene cues should support spatial orienting of attention. In the other half (32 target objects, four foils), the object appeared at an unlearned, invalidly cued location (invalid), in the opposite hemifield. Scenes and object locations were counterbalanced across participants so that objects were equally likely to occur on the left and right sides, and in valid and invalid cueing conditions. The LTM-guided attention task involved a straightforward target-detection task requiring rapid responses. To investigate LTM-guided attention within this context, we examined response times. Trials were excluded if RTs were below 200 ms or above two SD from the mean. Additionally, we computed the false alarm rate based on foil trials.

Explicit retrieval. Upon completing the LTM-guided attention task, participants were evaluated on their explicit memory content from the learning session. We tested 72 explicit associations between objects and scenes, either starting from the object (object-cued condition; n = 36) or the scene (scene-cued condition; n = 36). Object- and scene-cued conditions were counterbalanced across participants. One condition concerned both the location and identity of the object associated with the scene (scene-cued), while the other concerned both the object location and the identity of the scene associated with it (object-cued). This variation from the previously published paradigm was added to test for possible differences in information retrieval performance depending on the cue provided, either the object or the context (scene), given the known dissociation in explicit recall between objects and scenes (for example, ref. 63).

For the scene-cued condition, the 36 studied object–scene associations were tested in a randomized order. In each trial, a scene appeared without the embedded object (Fig. 3*A*). Participants were asked to click with the mouse cursor in the remembered object location within a 2-min time window. Following their response, they rated their confidence in locating the object by clicking one of three boxes labeled 1 "not at all confident," 2 "fairly confident," or 3 "very confident." A blank fixation period (1,000 to 1,500 ms) followed this rating. Afterward, four objects appeared at the center of the four quadrants of the screen (each within a transparent box of 150 × 150 pixels). Participants chose the object they remembered as associated with the scene in this 4AFC

recognition task and clicked it. For all trials, the competing objects were previously associated with other scenes, drawn randomly from the pool of all objects. Each object appeared as the target associated with the scene only once but could appear as a competing item in other randomly assigned scenes. Participants again rated their confidence level in their memory for object identity. No feedback was provided in this phase.

The object-cued condition followed the same experimental design. However, in this condition, the object appeared first at the center of a black screen. Then, participants were asked to click on the remembered object location (still on the black screen). Right after, they rated their confidence level by choosing among the three alternatives. After a blank fixation period, four scenes appeared at the centers of the four quadrants of the screen (each within a transparent 150 × 150-pixel box). Participants chose the scene they remembered to be associated with the object and rated their confidence level.

As a measure of explicit contextual memory for object location within a scene, we analyzed the mean distance between the retrieved location and the actual object location (in pixels). The mean accuracy in the two 4AFC tasks provided a measure of explicit contextual memory for object identity and scene identity. Performance on confidence ratings was not within the scope of this paper; therefore, we did not conduct analyses of this measure.

Behavioral data were analyzed using JAMOVI (version 2.3.21.0).

Apparatus. The tasks were programmed using Presentation (Neurobehavioural Systems, Albany, NY). A personal computer controlled the stimulus displays and collected the responses. The stimuli were displayed on a 24-inch monitor with a resolution of 1,028 by 768 pixels and a 60-Hz refresh rate.

Neuroimaging.

Data acquisition. Each participant underwent a 3D T1-weighted anatomical scan using a 1.5 T Philips Achieva scanner. For the 3D T1-weighted anatomical scan, a 3D-FFE sequence was used (Flip angle = 8°, TE = 3.2 ms, TR = 7.2 ms, matrix: 256 × 232; slice thickness = 1 mm, interslice gap = 0 mm; voxel size = 1 × 1 × 1 mm). Image acquisition quality was evaluated, and VBM was performed to assess regional gray matter volume and voxel-wise density differences between the HS and control groups (*SI Appendix*).

Hippocampal subfields and amygdala segmentation. We used FreeSurfer version 7.4.1 (https://surfer.nmr.mgh.harvard.edu/) recon-all function to automatically skull strip and segment cortical and subcortical volumes from the T1-weighted structural scans, which has been shown to have acceptable scan–rescan and test–retest reliability (64, 65) and comparable accuracy to manual labeling techniques (66, 67). Using the FreeView image viewer, all cortical and subcortical outputs were visually inspected to quality-check for processing and segmentation errors. The segmentation process was carried out on a MacBook Pro with an Apple M2 Pro chip, 16 GB of RAM, and macOS Ventura 13.5.1. The hippocampal subfield volumes and amygdala subregions (in mm^3) were extracted for subsequent analyses. The anatomical MRI data were first segmented to obtain volume values (in mm^3) using the recon-all function in FreeSurfer version 7.4.1. For the hippocampus, volumetric estimates were extracted bilaterally (left and right hemispheres) for the head and body of CA1, CA3 (including CA2/3), CA4, and the dentate gyrus molecular and granule cell layers (GCMLDG). For the amygdala, bilateral volumes were obtained for the lateral, basal, accessory basal, and central nuclei, as well as the corticoamygdaloid transition. Notably, subfield segmentations were independently reviewed by multiple coauthors in accordance with current quality-control recommendations. In addition, as an external validity check, we confirmed, through statistical comparisons, that subfields known to be most affected by HS—particularly CA1—showed the expected volumetric differences between patients and controls, which were consistently modulated by the side of HS (*SI Appendix*). Nevertheless, subfield volumes (e.g., molecular layer, GCMLDG) were derived using FreeSurfer's atlas-based probabilistic segmentation. Given the standard-resolution 1.5T T1 acquisitions, these measures should be interpreted as model-based estimates rather than direct delineations of anatomical boundaries.

Hierarchical Clustering. By applying the hierarchical clustering approach, we explored patterns of structural covariance between the LTM-guided attention index and hippocampus subfield volumes in HC and tested whether these covariance patterns differed in patients with HS. Hierarchical clustering identifies natural groupings or patterns in the data without requiring prior hypotheses. This can reveal complex relationships between variables that classic inferential and bivariate statistics might overlook. In the present study, this was particularly useful, as we do not have specific hypotheses regarding hippocampal subfields and sectors (body-head) clustering with the LTM-guided attention index. Furthermore, unlike bivariate approaches that evaluate isolated structure–function associations, hierarchical clustering leverages the full multivariate structure of the data, enabling the identification of brain–behavior patterns that would otherwise remain undetected when variables are analyzed independently. This approach not only mitigates the inflation of type I error inherent in multiple-hypothesis testing of bivariate correlations but also provides a more ecologically valid representation of hippocampal anatomo-functional organization in LTM-guided attention, which emerges from coordinated interactions between subfields rather than from isolated regional effects (e.g., ref. 34). Importantly, while clustering itself is descriptive, we employed inferential statistical methods to test whether the resulting pattern differed significantly between groups.

We performed a hierarchical clustering analysis separately for each group using the AGglomerative NESting (AGNES) clustering (68) using the cluster package (69). The AGNES method provides a natural way to visualize relationships at multiple levels of similarity (i.e., dendrogram), which aligns well with the hierarchical organization often observed in neuroanatomical and neurofunctional data. Previous neuroimaging studies employing the same experimental task as the present study have demonstrated an association between LTM-guided attention and the left hippocampus (8, 12). Accordingly, for each group, the model included the LTM-guided attention index together with the volumes of the eight subfields of the left hippocampus. Given that studies using similar tasks have also reported right hippocampal involvement (16), the analyses likewise incorporated the eight subfields of the right hippocampus. To provide a control condition for the potential covariance between LTM-guided attention and hippocampal subfields, we repeated the analyses, including the LTM-guided attention index and the volumes of the five subregions of both the left and right amygdala, a region not expected to contribute to this type of LTM-guided attention. Initially, relevant variables were standardized using z-score normalization to ensure comparability across different scales (brain region volumes and LTM-guided attention index). Then, nonparametric correlation matrices were computed to assess associations between variables separately for the three groups. These correlation matrices were transformed into distance matrices by computing the dissimilarity as "1–correlation coefficient" (according to the method described in https://bio723-class.github.io/Bio723-book/clustering-in-r.html). Hierarchical clustering was performed using Ward's method (ward.D2), which minimizes intracluster variance, making it especially appropriate for our dataset, which includes interrelated gray matter regions (*SI Appendix*, for an evaluation of result stability across different clustering methods). Dendrograms were generated to visualize the hierarchical structure of the data, enabling the identification of potential clusters. Then, we cut the dendrogram to $K = 2$ to reflect the anatomical constraint (i.e., left–right hippocampal regions). Indeed, we assume that the left and right hippocampal subfields would be separated, at least in HC. To test the validity of our dendrograms empirically, we computed the DB index (38), which assesses both the compactness and separation of clusters. Lower values indicate better clustering quality, as the elements within the clusters are more similar to each other and more dissimilar to those in other clusters (70, 71). DB values close to or below 1 typically indicate good clustering quality. Finally, we quantified the similarity between dendrogram structures across the three groups using the BHG index (39, 40), implemented in the R Library dendextend (72). The BHG index evaluates the agreement between two sets of clusters by comparing the pairwise distances of data points within each clustering. The range of the BHG index is typically from −1 to 1, where 0 indicates absence of concordance, and +1 indicates perfect agreement. To assess the statistical significance of similarities among the three dendrogram structures, we employed a permutation approach with 10,000 iterations, in which group labels were randomly shuffled for each iteration. The null hypothesis assumes that any observed differences in clustering structures between groups arise by chance alone. Specifically, for each pairwise comparison, we first pooled all subjects from the two groups being compared. Next, participants were randomly reassigned to two new groups while preserving the original group sizes. We then applied z-score standardization within each permuted group and subsequently computed hierarchical clustering dendrograms. Finally, in each iteration, the BHG index was calculated, generating an empirical null distribution of BHG values under the assumption of no systematic group differences,

against which the observed BHG was compared. One-tailed empirical *P*-values were calculated from this distribution as the proportion of permuted BHG values equal to or smaller than the observed BHG value. A significant *P*-value ($P < 0.05$) indicates that the observed clustering similarity is lower than expected under random group assignment, providing evidence for between-groups differences. Conversely, a nonsignificant *P*-value indicates insufficient evidence to conclude that clustering structures differ from what is expected by chance.

To illustrate the differences between group datasets in hierarchical clustering, we have included tanglegrams generated using the dendextend library in *R* (72). A tanglegram is a visual tool that compares two dendrograms by connecting corresponding leaves with colored lines, while branches leading to distinct subtrees are marked with dashed lines. This visualization helps assess the similarity and alignment between two hierarchical clustering results. The connecting lines indicate whether clusters or elements are preserved across the dendrograms.

Data, Materials, and Software Availability. The data generated in this study are available under restricted access as they contain information (age, gender, education level, and other clinical information) that could compromise research participant privacy/consent. Access can be obtained on request from the corresponding author (gerardo.salvato@unipv.it).

ACKNOWLEDGMENTS. This project was funded by the "Ricerca Finalizzata Giovani Ricercatori" Grant from the Italian Ministry of Health to G.S. (project PI) and M.Berl. (code: GR-2019-12369878).

Author affiliations: [a]Department of Brain and Behavioral Sciences, University of Pavia, Pavia 27100, Italy; [b]Cognitive Neuropsychology Centre, Azienda Socio-Sanitaria Territoriale "Grande Ospedale Metropolitano" Niguarda, Milano 20162, Italy; [c]NeuroMi, Milan Center for Neuroscience, Milano 20126, Italy; [d]Claudio Munari Epilepsy Surgery Centre, Azienda Socio-Sanitaria Territoriale "Grande Ospedale Metropolitano" Niguarda, Milano 20126, Italy; [e]Department of Medicine and Surgery, Unit of Neuroscience, University of Parma, Parma 43121, Italy; [f]Department of Neuroradiology, Azienda Socio-Sanitaria Territoriale "Grande Ospedale Metropolitano" Niguarda, Milano 20162, Italy; [g]Pathological anatomy histology and cytogenetics, Azienda Socio-Sanitaria Territoriale "Grande Ospedale Metropolitano" Niguarda, Milano 20162, Italy; [h]Department of Humanities, University of Urbino Carlo Bo, Urbino 61029, Italy; [i]Institute of Cognitive Neuroscience University College London, London WC1E 6BT, United Kingdom; [j]Wu Tsai Institute and Department of Psychology, Yale University, New Haven, CT 06510; and [k]Center of Clinical Developmental Neuropsychology, Azienda Sanitaria Territoriale Pesaro-Urbino, Pesaro 61122, Italy

Author contributions: G.S., A.C.N., and M. Berlingeri designed research; G.D.M., C.B., P.S., L.T., F.C., L.C., S.A.C.S., M.P., M. Bramerio, and M.C. performed research; T.F., M.C. M. Berlingeri analyzed data; and G.S., L.T., F.C., L.C., S.A.C.S., M.P., M.C., E.Z.P., A.C.N., M. Berlingeri, and G.B. wrote the paper.

1. M. Bar, The proactive brain: Memory for predictions. *Philos. Trans. R. Soc. B Biol. Sci.* **364**, 1235–1243 (2009).
2. M. M. Chun, M. K. Johnson, Memory: Enduring traces of perceptual and reflective attention. *Neuron* **72**, 520–535 (2011).
3. N. I. Córdova, N. B. Turk-Browne, M. Aly, Focusing on what matters: Modulation of the human hippocampus by relational attention. *Hippocampus* **29**, 1025–1037 (2019).
4. J. B. Hutchinson, N. B. Turk-Browne, Memory-guided attention: Control from multiple memory systems. *Trends Cogn. Sci.* **16**, 576–579 (2012).
5. A. C. K. Nobre, M.-M. Mesulam, "Large-scale networks for attentional biases" in *The Oxford Handbook of Attention*, A. C. K. Nobre, S. Kastner, Eds. (Oxford University Press, 2014).
6. A. C. Nobre, M. G. Stokes, Premembering experience: A hierarchy of time-scales for proactive attention. *Neuron* **104**, 132–146 (2019).
7. J. J. Summerfield, A. Rao, N. Garside, A. C. Nobre, Biasing perception by spatial long-term memory. *J. Neurosci.* **31**, 14952–14960 (2011).
8. J. J. Summerfield, J. Lepsien, D. R. Gitelman, M. M. Mesulam, A. C. Nobre, Orienting attention based on long-term memory experience. *Neuron* **49**, 905–916 (2006).
9. G. Salvato, E. Z. Patai, T. McCloud, A. C. Nobre, Apolipoprotein ε4 breaks the association between declarative long-term memory and memory-based orienting of spatial attention in middle-aged individuals. *Cortex* **82**, 206–216 (2016).
10. G. Salvato, E. Z. Patai, A. C. Nobre, Preserved memory-based orienting of attention with impaired explicit memory in healthy ageing. *Cortex* **74**, 67–78 (2016).
11. E. Z. Patai, S. Doallo, A. C. Nobre, Long-term memories bias sensitivity and target selection in complex scenes. *J. Cogn. Neurosci.* **24**, 2281–2291 (2012).
12. M. G. Stokes, K. Atherton, E. Z. Patai, A. C. Nobre, Long-term memory prepares neural activity for perception. *Proc. Natl. Acad. Sci. U.S.A.* **109**, E360–E367 (2012).
13. S. Doallo, E. Z. Patai, A. C., Nobre Reward Associations magnify memory-based biases on perception. *J. Cogn. Neurosci.* **25**, 245–257 (2013).
14. M. Fischer, M. Moscovitch, C. Alain, A systematic review and meta-analysis of memory-guided attention: Frontal and parietal activation suggests involvement of fronto-parietal networks. *Wiley Interdiscip. Rev. Cogn. Sci.* **12**, e1546 (2021).
15. M. L. Rosen, C. E. Stern, S. W. Michalka, K. J. Devaney, D. C. Somers, Cognitive control network contributions to memory-guided visual attention. *Cereb. Cortex* **26**, 2059–2073 (2016).
16. E. Günseli, M. Aly, Preparation for upcoming attentional states in the hippocampus and medial prefrontal cortex. *Elife* **9**, e53191 (2020).
17. M. A. Rosero *et al.*, Memory-guided attention: Bilateral hippocampal volume positively predicts implicit contextual learning. *Brain Struct. Funct.* **224**, 1999–2008 (2019).
18. M. M. Chun, Contextual cueing of visual attention. *Trends Cogn. Sci.* **4**, 170–178 (2000).
19. M. M. Chun, Y. Jiang, Contextual cueing: Implicit learning and memory of visual context guides spatial attention. *Cogn. Psychol.* **36**, 28–71 (1998).
20. A. R. Preston, J. D. E. Gabrieli, Dissociation between explicit memory and configural memory in the human medial temporal lobe. *Cereb. Cortex* **18**, 2192–2207 (2008).
21. C. E. Westerberg, B. B. Miller, P. J. Reber, N. J. Cohen, K. A. Paller, Neural correlates of contextual cueing are modulated by explicit learning. *Neuropsychologia* **49**, 3439–3447 (2011).
22. M. L. Rosen, C. E. Stern, K. J. Devaney, D. C. Somers, Cortical and subcortical contributions to long-term memory-guided visuospatial attention. *Cereb. Cortex* **28**, 2935–2947 (2018).
23. A. J. Greene, W. L. Gross, C. L. Elsinger, S. M. Rao, Hippocampal differentiation without recognition: An fMRI analysis of the contextual cueing task. *Learn. Mem.* **14**, 548–553 (2007).
24. J. H. Howard Jr., D. V. Howard, N. A. Dennis, H. Yankovich, C. J. Vaidya, Implicit spatial contextual learning in healthy aging. *Neuropsychology* **18**, 124–134 (2004).
25. D. Hassabis, E. A. Maguire, The construction system of the brain. *Philos. Trans. R. Soc. B Biol. Sci.* **364**, 1263–1271 (2009).
26. M. Chaumon, D. Hasboun, M. Baulac, C. Adam, C. Tallon-Baudry, Unconscious contextual memory affects early responses in the anterior temporal lobe. *Brain Res.* **1285**, 77–87 (2009).
27. M. M. Chun, E. A. Phelps, Memory deficits for implicit contextual information in amnesic subjects with hippocampal damage. *Nat. Neurosci.* **2**, 844–847 (1999).
28. J. R. Manns, L. R. Squire, Perceptual learning, awareness, and the hippocampus. *Hippocampus* **11**, 776–782 (2001).
29. E. Oudman, S. Van der Stigchel, A. J. Wester, R. P. C. Kessels, A. Postma, Intact memory for implicit contextual information in Korsakoff's amnesia. *Neuropsychologia* **49**, 2848–2855 (2011).
30. I. Blümcke *et al.*, International consensus classification of hippocampal sclerosis in temporal lobe epilepsy: A task force report from the ILAE Commission on diagnostic methods. *Epilepsia* **54**, 1315–1329 (2013).
31. J. H. Margerison, J. A. Corsellis, Epilepsy and the temporal lobes. A clinical, electroencephalographic and neuropathological study of the brain in epilepsy, with particular reference to the temporal lobes. *Brain* **89**, 499–530 (1966).
32. C. Helmstaedter, E. Kockelmann, Cognitive outcomes in patients with chronic temporal lobe epilepsy. *Epilepsia* **47**, 96–98 (2006).
33. C. M. Marques *et al.*, Cognitive decline in temporal lobe epilepsy due to unilateral hippocampal sclerosis. *Epilepsy Behav.* **10**, 477–485 (2007).
34. R. Coras *et al.*, Differential influence of hippocampal subfields to memory formation: Insights from patients with temporal lobe epilepsy. *Brain* **137**, 1945–1957 (2014).
35. K. Cao *et al.*, Identifying and validating subtypes of Parkinson's disease based on multimodal MRI data via hierarchical clustering analysis. *Front. Hum. Neurosci.* **16**, 919081 (2022).
36. J. Sheng *et al.*, Novel Alzheimer's disease subtypes based on functional brain connectivity in human connectome project. *Sci. Rep.* **14**, 14821 (2024).
37. M. Boly *et al.*, Hierarchical clustering of brain activity during human nonrapid eye movement sleep. *Proc. Natl. Acad. Sci. U.S.A.* **109**, 5856–5861 (2012).
38. D. L. Davies, D. W. Bouldin, A cluster separation measure. *IEEE Trans. Pattern Anal. Mach. Intell.* **PAMI-1**, 224–227 (1979).
39. F. B. Baker, Stability of two hierarchical grouping techniques case 1: Sensitivity to data errors. *J. Am. Stat. Assoc.* **69**, 440 (1974).
40. J. O. E. Remmers, A. J. Teuling, L. A. Melsen, Can model structure families be inferred from model output? *Environ. Model. Softw.* **133**, 104817 (2020).
41. N. Del Vecchio, J. Liporace, M. Nei, M. Sperling, J. Tracy, A dissociation between implicit and explicit verbal memory in left temporal lobe epilepsy. *Epilepsia* **45**, 1124–1133 (2004).
42. B. D. Bell, A. R. Giovagnoli, Recent innovative studies of memory in temporal lobe epilepsy. *Neuropsychol. Rev.* **17**, 455–476 (2007).
43. E. C. Leritz, L. J. Grande, R. M. Bauer, Temporal lobe epilepsy as a model to understand human memory: The distinction between explicit and implicit memory. *Epilepsy Behav.* **9**, 1–13 (2006).
44. A. P. Shimamura, L. R. Squire, Impaired priming of new associations in amnesia. *J. Exp. Psychol. Learn. Mem. Cogn.* **15**, 721–728 (1989).
45. B. R. Postle, S. Corkin, Impaired word-stem completion priming but intact perceptual identification priming with novel words: Evidence from the amnesic patient H.M. *Neuropsychologia* **36**, 421–440 (1998).
46. C. Bigras, P. K. Shear, J. Vannest, J. B. Allendorfer, J. P. Szaflarski, The effects of temporal lobe epilepsy on scene encoding. *Epilepsy Behav.* **26**, 11–21 (2013).
47. S. B. Bonelli *et al.*, Imaging memory in temporal lobe epilepsy: Predicting the effects of temporal lobe resection. *Brain* **133**, 1186–1199 (2010).
48. P. Figueiredo *et al.*, Adaptive visual memory reorganization in right medial temporal lobe epilepsy. *Epilepsia* **49**, 1395–1408 (2008).
49. A. J. Golby *et al.*, Memory lateralization in medial temporal lobe epilepsy assessed by functional MRI. *Epilepsia* **43**, 855–863 (2002).
50. C. Limotai *et al.*, Memory loss and memory reorganization patterns in temporal lobe epilepsy patients undergoing anterior temporal lobe resection, as demonstrated by pre-versus post-operative functional MRI. *J. Clin. Neurosci.* **55**, 38–44 (2018).
51. H. W. R. Powell *et al.*, Reorganization of verbal and nonverbal memory in temporal lobe epilepsy due to unilateral hippocampal sclerosis. *Epilepsia* **48**, 1512–1525 (2007).
52. M. P. Richardson, B. A. Strange, J. S. Duncan, R. J. Dolan, Preserved verbal memory function in left medial temporal pathology involves reorganisation of function to right medial temporal lobe. *Neuroimage* **20**, S112–S119 (2003).
53. J. Stretton *et al.*, Working memory network plasticity after anterior temporal lobe resection: A longitudinal functional magnetic resonance imaging study. *Brain* **137**, 1439–1453 (2014).
54. W. M. Kelley *et al.*, Hemispheric specialization in human dorsal frontal cortex and medial temporal lobe for verbal and nonverbal memory encoding. *Neuron* **20**, 927–936 (1998).
55. H. Kim, S. Yi, E. I. Son, J. Kim, Material-specific memory in temporal lobe epilepsy: Effects of seizure laterality and language dominance. *Neuropsychology* **17**, 59–68 (2003).
56. M. St-Laurent *et al.*, Using multivariate data reduction to predict postsurgery memory decline in patients with mesial temporal lobe epilepsy. *Epilepsy Behav.* **31**, 220–227 (2014).

57. D. E. Hannula, L. A. Libby, A. P. Yonelinas, C. Ranganath, Medial temporal lobe contributions to cued retrieval of items and contexts. *Neuropsychologia* **51**, 2322–2332 (2013).
58. D. E. Hannula, C. Ranganath, The eyes have it: Hippocampal activity predicts expression of memory in eye movements. *Neuron* **63**, 592–599 (2009).
59. M. F. Folstein, S. E. Folstein, P. R. McHugh, Mini-mental state. *J. Psychiatr. Res.* **12**, 189–198 (1975).
60. T. Judd, K. Ehinger, F. Durand, A. Torralba, "Learning to predict where humans look" in *2009 IEEE 12th International Conference on Computer Vision* (IEEE, 2009), pp. 2106–2113.
61. B. C. Russell, A. Torralba, K. P. Murphy, W. T. Freeman, LabelMe: A database and web-based tool for image annotation. *Int. J. Comput. Vis.* **77**, 157–173 (2008).
62. J. Xiao, J. Hays, K. A. Ehinger, A. Oliva, A. Torralba, "SUN database: Large-scale scene recognition from abbey to zoo" in *2010 IEEE Computer Society Conference on Computer Vision and Pattern Recognition* (IEEE, 2010), pp. 3485–3492.
63. W. A. Bainbridge, E. H. Hall, C. I. Baker, Distinct representational structure and localization for visual encoding and recall during visual imagery. *Cereb. Cortex* **31**, 1898–1913 (2021).
64. E. M. Brown *et al.*, Test-retest reliability of FreeSurfer automated hippocampal subfield segmentation within and across scanners. *Neuroimage* **210**, 116563 (2020).
65. X. Han *et al.*, Reliability of MRI-derived measurements of human cerebral cortical thickness: The effects of field strength, scanner upgrade and manufacturer. *NeuroImage* **32**, 180–194 (2006).
66. A. M. Dale, B. Fischl, M. I. Sereno, Cortical surface-based analysis: I. Segmentation and surface reconstruction. *NeuroImage* **9**, 179–194 (1999).
67. B. Fischl *et al.*, Whole brain segmentation. *Neuron* **33**, 341–355 (2002).
68. J. E. Gentle, L. Kaufman, P. J. Rousseuw, Finding groups in data: An introduction to cluster analysis. *Biometrics* **47**, 788 (1991).
69. M. Maechler, P. Rousseeuw, A. Struyf, M. Hubert, Cluster: "Finding groups in data": Cluster analysis extended Rousseeuw et al. CRAN: Contributed Packages. https://doi.org/10.32614/CRAN.package.cluster. Deposited 12 April 1999.
70. N. Tomašev, M. Radovanović, "Clustering evaluation in high-dimensional data" in *Unsupervised Learning Algorithms*, M. E. Celebi, K. Aydin, Eds. (Springer International Publishing, 2016), pp. 71–107.
71. S. Yue, J.-S. Wang, T. Wu, H. Wang, A new separation measure for improving the effectiveness of validity indices. *Inf. Sci.* **180**, 748–764 (2010).
72. T. Galili, Dendextend: An R package for visualizing, adjusting and comparing trees of hierarchical clustering. *Bioinformatics* **31**, 3718–3720 (2015).